Acta Cryst. (1983). B**39**, 54–61

Crystalline-State Reaction of Cobaloxime Complexes by X-ray Exposure. IV. A Relationship between the Reaction Rate and the Volume of the Cavity for the Reactive Group

BY YUJI OHASHI,† AKIRA UCHIDA AND YOSHIO SASADA

Laboratory of Chemistry for Natural Products, Tokyo Institute of Technology, Nagatsuta, Midori-ku, Yokohama 227, *Japan*

AND YOSHIAKI OHGO

Niigata College of Pharmacy, 5829 *Kamishinei-cho, Niigata* 950-21, *Japan*

(*Received* 12 *July* 1982; *accepted* 23 *August* 1982)

Abstract

Crystals of [(*R*)-1-cyanoethyl]bis(dimethylglyoximato)(4-pyridinecarbonitrile)cobalt(III) (dimethylglyoximato = 2,3-butanedione dioximato), $C_{17}H_{22}CoN_7O_4$, $[Co(C_3H_4N)(C_6H_4N_2)(C_4H_7N_2O_2)_2]$, reveal crystalline-state racemization on exposure to X-rays. At the initial stage, the crystal is triclinic, space group $P\bar{1}$, with a = 9·313 (3), b = 15·564 (5), c = 7·764 (2) Å, α = 96·76 (2), β = 102·03 (3), γ = 111·80 (3)°, V = 998·1 (6) Å^3, D_m = 1·49, D_c = 1·491 g cm^{-3} for Z = 2, and μ(Mo $K\alpha$) = 9·38 cm^{-1}. (R = 0·064 for 3334 observed reflections.) The two crystallographically independent molecules are related by a pseudo inversion. On irradiation with X-rays, the unit-cell dimensions gradually change, converging to a = 9·300 (2), b = 15·283 (3), c = 7·808 (1) Å, α = 96·61 (1), β = 101·25 (1), γ = 111·12 (1)° and V = 994·3 (3) Å^3 without degradation of crystallinity. (R = 0·046 for 3382 observed reflections.) The chiral cyanoethyl group in one of the two molecules at the initial stage converts its configuration so that a crystallographic inversion center appears between the two molecules at the final stage. The space group is transformed to $P\bar{1}$. The cavity of the cyanoethyl group clearly indicates which of the two cyanoethyl groups at the initial stage is reactive. The volume of the cavity for the reactive cyanoethyl group (10·37 Å^3) is greater than that for the non-reactive cyanoethyl group (7·97 Å^3). The reaction follows approximate first-order kinetics, the rate constant being 1·65 × 10^{-6} s^{-1}. Comparison of the rate constants of related cobaloxime complexes clearly indicates that there is a positive correlation with the volume of the cavity.

Introduction

The chiral 1-cyanoethyl group, $-C^*H(CH_3)CN$, bonded to the Co atom in crystals of bis(dimethylglyoximato)cobalt (hereafter abbreviated as cobaloxime) has been found to be racemized by X-ray exposure without degradation of the crystallinity (Ohashi & Sasada, 1977). Such a remarkable type of solid-state reaction makes possible direct observation of the chemical reaction and detailed understanding of the correlation between the reactant and its environment. We have called this a crystalline-state reaction and have been studying it extensively.

In crystals of [(*R*)-1-cyanoethyl][(*S*)-α-methylbenzylamine]cobaloxime [(1), *R*-cn-*S*-mba, shown in Fig. 1], and its diastereomer [(2), *S*-cn-*S*-mba], the ordered enantiomers of the cyanoethyl group are converted into disordered racemates (Ohashi, Sasada & Ohgo, 1978*a*,*b*; Ohashi, Yanagi, Kurihara, Sasada & Ohgo, 1981). For the crystal of [(*S*)-1-cyanoethyl](pyridine)cobaloxime [(3), *S*-cn-py], on the other hand, one of the two crystallographically independent cyanoethyl groups is transformed into the opposite configuration and an inversion center appears between them (Ohashi, Yanagi, Kurihara, Sasada & Ohgo,

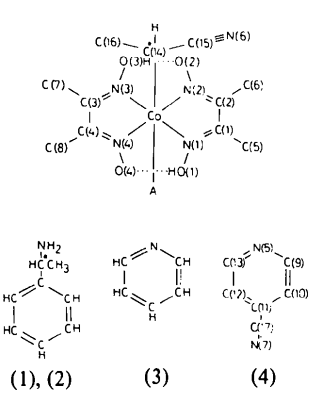

(1), (2) (3) (4)

Fig. 1. Cobaloxime complexes including the cyanoethyl group as an axial ligand with the atomic numbering: (1) and (2) *S*-α-methylbenzylamine (*R*-cn-*S*-mba and *S*-cn-*S*-mba); (3) pyridine (*S*-cn-py); (4) 4-pyridinecarbonitrile (*R*-cn-cnpy).

† To whom correspondence should be addressed.

0567-7408/83/010054-08$01.50

1982). This is a new mode of reaction which is different from that of the first two examples; that is, the ordered enantiomeric cyanoethyl groups are converted into ordered racemic ones.

The change of the unit-cell dimensions caused by the racemization follows approximate first-order kinetics. The rate constants for the three crystals are 2·10–3·28 × 10^{-6} s^{-1}. Although the reaction rate seemed to be dependent on the crystal structure, the quantitative relation has not yet been obtained. This might be due to the different reaction mechanisms among the three crystals. Recently, we have prepared several cobaloxime complexes containing 4-substituted pyridine as an axial amine ligand. The present paper reports the mechanism of the order-to-order racemization of the crystal of [(*R*)-1-cyanoethyl](4-pyridinecarbonitrile)-cobaloxime [(4), *R*-cn-cnpy]. Another example of crystalline-state racemization is observed in the cobaloxime crystals that contain the methoxy-carbonylethyl group, $-C^*H(CH_3)CO_2CH_3$, as a chiral group instead of the cyanoethyl group (Kurihara, Ohashi & Sasada, 1982; Ohashi, Kurihara, Sasada & Ohgo, 1981).

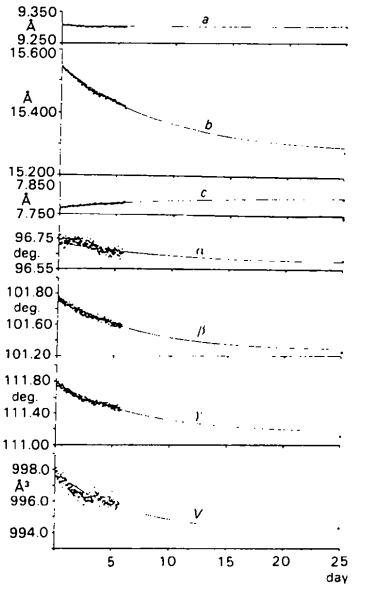

Fig. 2. The change of the unit-cell dimensions on X-ray exposure at room temperature. First-order reaction curves are obtained by least-squares fitting using the experimental values.

Experimental

Dark-red crystals of *R*-cn-cnpy were obtained from an aqueous methanol solution. Preliminary cell dimensions and the space group were deduced from photographs. A crystal 0·4 × 0·4 × 0·3 mm, selected carefully on a microscope, was mounted on a Rigaku four-circle diffractometer. Mo $K\alpha$ radiation monochromated by graphite was used (40 kV, 20 mA, λ = 0·71069 Å). The unit-cell dimensions were obtained by means of the least-squares technique with 21 reflections in the range $25° \leq 2\theta \leq 30°$. The determination of the cell dimensions was repeated continuously in the early stages, to register their change; this took about 40 min for each cycle. The exposure time was recorded by a clock which ran when the X-ray window-shutter was open. After a week the rate of the change in the unit-cell dimensions decreased so that the monitoring was performed once a day. The changes were within experimental error after three weeks. Fig. 2 shows the changes of a, b, c, α, β, γ and V with the exposure time.

Three-dimensional intensity data were collected at the initial and final stages. Intensities of reflections in the range $2\theta \leq 50°$ for the initial stage and $2\theta \leq 55°$ for the final stage were measured by means of an $\omega/2\theta$ scan with a scanning rate of 8° (2θ) min^{-1} and a scan width of $(1·0 + 0·35 \tan\theta)°$. Stationary background counts were accumulated for 5 s before and after each scan. In the course of the intensity-data collection the orientation matrix was redetermined if the intensities of three monitor reflections varied significantly (greater than 8σ). Before and after the data collection at the initial stage, the unit-cell dimensions changed significantly; their average values (a = 9·300, b = 15·542, c = 7·762 Å, α = 96·82, β = 101·80 and γ = 111·73°) were used throughout the structure determination.

Intensity statistics indicated that the structure at the final stage has an inversion center and the space group has changed from $P1$ to $P\bar{1}$. At first, the structure of the final stage was solved by the direct method using the program *MULTAN* 78 (Main, Hull, Lessinger, Germain, Declercq & Woolfson, 1978) and refined by block-diagonal least squares using a modified *HBLS* program (Ohashi, 1975). All the H atoms were found on a difference map. The final refinement was made with anisotropic and isotropic thermal parameters for non-hydrogen and H atoms, respectively. The weighting scheme was $w = [\sigma^2(|F_o|) + a|F_o|^2]^{-1}$ where a = 0·0009. In the final difference map no peaks higher than 0·6 e $Å^{-3}$ were found except for two peaks around the Co atom. The final R value was 0·064 for 3334 observed reflections.

Starting from the structural parameters at the final stage, the structure of the initial stage was refined by constrained full-matrix least squares using the program *SHELX* 76 (Sheldrick, 1976), to avoid parameter interaction between the two crystallographically independent molecules. The final refinement was made without constraint for non-hydrogen atoms, the H atoms being geometrically fixed at 1·08 Å from the bonded atoms. The value of a in the weighting scheme was 0·00156. There were no residual peaks higher than 0·5 e $Å^{-3}$ in the difference map. The final R value was 0·046 for 3382 observed reflections.

Table 1. *Final atomic coordinates* ($\times 10^4$) *and equivalent isotropic thermal parameters* (Å^2) *for non-hydrogen atoms at the initial stage*

$B_{eq} = \frac{1}{3} \sum_i \sum_j B_{ij} a_i^* a_j^* \mathbf{a}_i . \mathbf{a}_j$.

	x	y	z	B_{eq}
Co(*A*)	4219 (1)	7166 (1)	3245 (1)	2·3
N(1*A*)	2534 (5)	6102 (3)	3481 (5)	2·2
N(2*A*)	4014 (5)	6293 (3)	1213 (6)	2·7
N(3*A*)	5961 (5)	8221 (3)	3013 (6)	2·9
N(4*A*)	4436 (6)	8031 (3)	5291 (6)	3·0
O(1*A*)	1830 (5)	6134 (3)	4859 (6)	3·8
O(2*A*)	4941 (5)	6522 (3)	85 (5)	3·9
O(3*A*)	6635 (5)	8222 (4)	1626 (6)	4·1
O(4*A*)	3476 (5)	7802 (3)	6350 (5)	3·6
C(1*A*)	1990 (6)	5339 (4)	2256 (8)	3·1
C(2*A*)	2880 (8)	5446 (4)	835 (8)	3·3
C(3*A*)	6449 (7)	8995 (4)	4230 (9)	3·4
C(4*A*)	5520 (7)	8877 (4)	5569 (8)	3·2
C(5*A*)	657 (8)	4443 (4)	2341 (12)	4·6
C(6*A*)	2587 (10)	4720 (5)	−771 (12)	5·4
C(7*A*)	7795 (8)	9855 (6)	4162 (15)	5·9
C(8*A*)	5833 (9)	9636 (5)	7135 (10)	4·4
N(5*A*)	2629 (4)	7610 (2)	1717 (4)	1·5
C(9*A*)	2808 (5)	7823 (3)	98 (6)	2·5
C(10*A*)	1832 (6)	8196 (3)	−896 (6)	3·0
C(11*A*)	660 (5)	8317 (3)	−166 (6)	2·8
C(17*A*)	−363 (7)	8752 (4)	−1086 (7)	4·2
N(7*A*)	−1053 (8)	9139 (5)	−1783 (8)	6·7
C(12*A*)	338 (5)	8016 (3)	1390 (6)	2·9
C(13*A*)	1381 (5)	7662 (3)	2280 (6)	2·5
C(14*A*)	5795 (7)	6714 (4)	4667 (7)	4·0
C(15*A*)	7379 (6)	7120 (4)	4541 (6)	3·4
N(6*A*)	8692 (7)	7447 (6)	4429 (8)	6·5
C(16*A*)	5754 (7)	6723 (5)	6594 (7)	3·8
Co(*B*)	5779 (1)	2830 (1)	6758 (1)	2·4
N(1*B*)	7520 (6)	3889 (4)	6553 (7)	3·7
N(2*B*)	5939 (7)	3701 (4)	8775 (6)	3·7
N(3*B*)	4060 (6)	1758 (4)	6961 (7)	3·4
N(4*B*)	5594 (5)	1959 (3)	4727 (6)	2·7
O(1*B*)	8227 (5)	3912 (3)	5175 (7)	4·3
O(2*B*)	4975 (7)	3439 (4)	9875 (7)	5·3
O(3*B*)	3362 (5)	1767 (4)	8343 (7)	4·6
O(4*B*)	6533 (5)	2203 (3)	3611 (5)	4·0
C(1*B*)	7971 (8)	4663 (4)	7727 (8)	3·6
C(2*B*)	7080 (8)	4548 (5)	9043 (9)	4·2
C(3*B*)	3560 (6)	996 (4)	5734 (8)	3·2
C(4*B*)	4413 (6)	1115 (4)	4392 (7)	3·1
C(5*B*)	9301 (10)	5584 (6)	7770 (12)	5·4
C(6*B*)	7450 (12)	5318 (6)	10626 (11)	6·0
C(7*B*)	2176 (8)	74 (4)	5655 (11)	4·6
C(8*B*)	4051 (8)	364 (5)	2700 (9)	4·5
N(5*B*)	7390 (5)	2442 (3)	8283 (6)	3·7
C(9*B*)	7238 (6)	2164 (4)	9797 (6)	3·4
C(10*B*)	8208 (6)	1826 (4)	10802 (6)	3·4
C(11*B*)	9435 (5)	1715 (3)	10211 (7)	3·1
C(17*B*)	10358 (6)	1290 (4)	11188 (8)	4·1
N(7*B*)	11083 (7)	950 (5)	12002 (9)	6·2
C(12*B*)	9567 (6)	1958 (4)	8585 (7)	3·4
C(13*B*)	8574 (6)	2304 (4)	7652 (7)	3·3
C(14*B*)	4247 (5)	3240 (4)	5043 (7)	3·2
C(15*B*)	2666 (7)	2923 (4)	5433 (8)	3·9
N(6*B*)	1418 (7)	2675 (5)	5505 (9)	6·9
C(16*B*)	4768 (9)	4212 (6)	4722 (14)	7·1

Atomic scattering factors including anomalous-dispersion terms were taken from *International Tables for X-ray Crystallography* (1974). The final atomic parameters for the non-hydrogen atoms at the initial and final stages are given in Tables 1 and 2, respectively.*

Table 2. *Final atomic coordinates* ($\times 10^5$ *for* Co; $\times 10^4$ *for* C, N *and* O) *and equivalent isotropic thermal parameters* (Å^2) *at the final stage*

$B_{eq} = \frac{1}{3} \sum_i \sum_j B_{ij} a_i^* a_j^* \mathbf{a}_i . \mathbf{a}_j$.

	x	y	z	B_{eq}
Co	42078 (5)	71344 (4)	32122 (6)	2·5
N(1)	2493 (4)	6066 (2)	3454 (4)	3·1
N(2)	3993 (4)	6258 (2)	1146 (4)	3·3
N(3)	5932 (4)	8201 (2)	2983 (4)	3·1
N(4)	4428 (4)	8005 (2)	5278 (4)	3·0
O(1)	1789 (3)	6070 (2)	4817 (4)	4·1
O(2)	4950 (4)	6520 (2)	66 (4)	4·5
O(3)	6620 (3)	8195 (2)	1619 (4)	4·4
O(4)	3458 (3)	7761 (2)	6355 (4)	3·8
C(1)	1980 (5)	5293 (3)	2221 (6)	3·6
C(2)	2865 (5)	5418 (3)	853 (6)	3·7
C(3)	6440 (4)	8964 (3)	4217 (6)	3·5
C(4)	5550 (4)	8847 (3)	5584 (5)	3·3
C(5)	658 (6)	4400 (3)	2248 (8)	5·2
C(6)	2547 (7)	4667 (4)	−751 (7)	5·6
C(7)	7805 (5)	9869 (4)	4268 (7)	5·3
C(8)	5848 (5)	9597 (4)	7160 (7)	4·7
N(5)	2626 (3)	7599 (2)	1750 (4)	2·5
C(9)	2800 (4)	7839 (3)	192 (5)	3·0
C(10)	1824 (5)	8200 (3)	−804 (5)	3·3
C(11)	618 (4)	8319 (3)	−141 (5)	3·0
C(17)	−372 (5)	8737 (3)	−1099 (6)	4·0
N(7)	−1091 (6)	9093 (4)	−1854 (7)	6·5
C(12)	401 (4)	8055 (3)	1446 (5)	3·1
C(13)	1420 (4)	7696 (3)	2355 (5)	2·9
C(14)	5707 (5)	6611 (4)	4622 (7)	4·5
C(15)	7345 (5)	7060 (3)	4534 (6)	3·9
N(6)	8626 (5)	7394 (4)	4542 (6)	6·3
C(16)	5590 (8)	6502 (6)	6425 (9)	8·2

Results and discussion

Reaction rate

Fig. 2 clearly shows that the change in the unit-cell dimensions of the crystal follows approximate first-order kinetics as observed in the crystals of *R*-cn-*S*-mba, *S*-cn-*S*-mba and *S*-cn-py. For the present crystal, the changes in the cell dimensions b, β, γ and V are significant. The rate constants, k_b, k_β, k_γ and k_V, were calculated to be $1{\cdot}40 \times 10^{-6}$, $1{\cdot}73 \times 10^{-6}$, $1{\cdot}63 \times 10^{-6}$ and $1{\cdot}84 \times 10^{-6}$ s^{-1}, respectively. The average, $1{\cdot}65 \times 10^{-6}$ s^{-1}, is smaller than the corresponding value, $2{\cdot}83 \times 10^{-6}$ s^{-1}, of the *S*-cn-py crystal.

* Lists of structure factors, anisotropic thermal parameters and H-atom parameters have been deposited with the British Library Lending Division as Supplementary Publication No. SUP 38123 (30 pp.). Copies may be obtained through The Executive Secretary, International Union of Crystallography, 5 Abbey Square, Chester CH1 2HU, England.

Crystal structure

The crystal structures at the initial and final stages are shown in Fig. 3. The crystal at the initial stage contains two crystallographically independent molecules, *A* and *B*. Hereafter the atoms and groups in either *A* or *B* are labelled *A* or *B*. The two molecules *A* and *B* are closely related by a pseudo inversion, except for the methyl groups [C(16*A*) and C(16*B*)] of the cyanoethyl groups. When the crystal is exposed to X-rays, C(16*B*) is transferred to a new position, C(16′), so that the cyanoethyl group *B* is converted from the *R* configuration to *S*. The configuration of the cyanoethyl group *A*, on the other hand, is unchanged. The pseudo inversion center then becomes a crystallographic inversion center. This indicates that the change is a conversion from an ordered enantiomeric structure to an ordered racemic one. Such an order-to-order racemization is essentially the same as that found in the crystal of *S*-cn-py. The racemic crystals of the present complexes were also prepared from aqueous methanol solution. They have the same cell dimensions and space group as the racemic crystal produced by X-ray exposure.

Molecular structure

Bond distances and angles at the initial and final stages are shown in Tables 3 and 4, respectively; corresponding values are not significantly different. However, the conformations of the two axial ligands differ significantly. The torsional angles C(15)–C(14)–Co–N(3) are 16·3 (5), 29·3 (4) and 14·0 (4)° and C(9)–N(5)–Co–N(3) are 50·8 (4), 46·1 (5) and 50·1 (3)° for the initial *A* and *B* and the final *A*′ molecules, respectively. The torsional angles of molecule *B* change markedly, whereas those of *A* change only slightly.

Structure around the cyanoethyl groups

Fig. 4 shows the crystal structure in the vicinity of the two cyanoethyl groups at the initial stage, viewed along the normal to the mean plane of the cobaloxime moiety *A*. The short interatomic distances are also given. The two cyanoethyl groups occupy the space between the two cobaloxime moieties and face each other. The mean planes of the cobaloximes are approximately parallel [the dihedral angle is 1·2 (2)°] and the distance between the two mean planes is 6·69 Å. The C(16*B*) methyl group has usual van der Waals contacts with cyanoethyl group *A* and prevents closer approach of molecules *A* and *B*. The Co(*A*)···Co(*B*) distance is 8·059 (1) Å. When C(16*B*) is transferred to the position C(16′) by X-ray exposure, the two molecules approach each other, resulting in a significant contraction of the crystal along the *b* axis, as shown in Fig. 2. The distance between the two Co atoms becomes 7·786 (1) Å, whereas the separation of the two mean planes, 6·662 (5) Å, is approximately the same as that of the initial stage.

It is noteworthy that C(16*A*) has an unusually short contact [2·98 (1) Å] with O(2*A*) of the neighboring molecule and the short contact is retained after the racemization. On the other hand, C(16*B*) has a fairly loose contact [3·88 (1) Å] with O(2*B*) of the neighboring molecule but has a short contact after the racemization [C(16′)···O(2) 3·01 (1) Å]. This is distinct from the racemization in the crystal of *S*-cn-py, in which C(16*B*), the methyl group of the reactive

Table 3. *Bond distances* (Å) *of the initial A and B and the final A′ molecules*

	A	*B*	*A′*
Co–N(1)	1·870 (5)	1·885 (6)	1·884 (4)
Co–N(2)	1·882 (5)	1·886 (6)	1·903 (4)
Co–N(3)	1·889 (5)	1·884 (5)	1·884 (4)
Co–N(4)	1·879 (6)	1·886 (5)	1·897 (4)
Co–N(5)	2·074 (4)	2·030 (5)	2·065 (3)
Co–C(14)	2·036 (7)	2·075 (6)	2·052 (6)
N(1)–O(1)	1·368 (7)	1·363 (8)	1·353 (5)
N(1)–C(1)	1·288 (8)	1·290 (9)	1·307 (6)
N(2)–O(2)	1·338 (7)	1·351 (9)	1·331 (5)
N(2)–C(2)	1·298 (9)	1·309 (10)	1·292 (6)
N(3)–O(3)	1·352 (8)	1·364 (8)	1·345 (5)
N(3)–C(3)	1·302 (9)	1·292 (8)	1·296 (6)
N(4)–O(4)	1·317 (7)	1·342 (7)	1·335 (5)
N(4)–C(4)	1·286 (9)	1·316 (8)	1·290 (6)
C(1)–C(2)	1·498 (10)	1·429 (10)	1·458 (7)
C(1)–C(5)	1·502 (11)	1·496 (12)	1·476 (8)
C(2)–C(6)	1·484 (12)	1·494 (13)	1·502 (8)
C(3)–C(4)	1·467 (10)	1·423 (9)	1·461 (6)
C(3)–C(7)	1·471 (13)	1·515 (11)	1·492 (7)
C(4)–C(8)	1·488 (11)	1·537 (10)	1·491 (7)
N(5)–C(9)	1·363 (6)	1·316 (8)	1·339 (5)
N(5)–C(13)	1·347 (6)	1·367 (8)	1·346 (5)
C(9)–C(10)	1·402 (7)	1·362 (9)	1·385 (6)
C(10)–C(11)	1·387 (8)	1·372 (8)	1·382 (6)
C(11)–C(17)	1·478 (9)	1·423 (8)	1·442 (6)
C(11)–C(12)	1·395 (7)	1·376 (8)	1·375 (6)
C(17)–N(7)	1·135 (10)	1·140 (10)	1·129 (8)
C(12)–C(13)	1·390 (7)	1·362 (8)	1·381 (6)
C(14)–C(15)	1·401 (9)	1·476 (9)	1·446 (8)
C(14)–C(16)	1·502 (10)	1·476 (12)	1·456 (11)
C(15)–N(6)	1·163 (11)	1·095 (11)	1·112 (8)

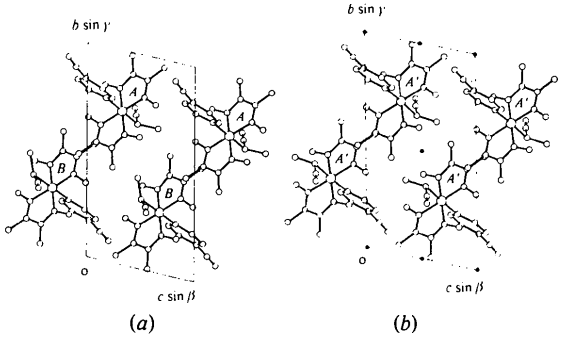

(*a*) (*b*)

Fig. 3. (*a*) Crystal structure at the initial stage viewed along the *a* axis. Two crystallographically independent molecules *A* and *B* are related by pseudo inversion. (*b*) Crystal structure at the final stage viewed along the *a* axis.

Table 4. *Bond angles* (°) *of the initial A and B and the final A' molecules*

	A	*B*	*A'*
N(1)–Co–N(2)	80·6 (2)	81·5 (3)	81·2 (2)
N(1)–Co–N(3)	178·3 (2)	179·0 (3)	179·6 (2)
N(1)–Co–N(4)	99·2 (2)	98·7 (2)	98·8 (2)
N(1)–Co–N(5)	91·8 (2)	88·4 (2)	90·2 (1)
N(1)–Co–C(14)	88·7 (2)	88·4 (2)	87·6 (2)
N(2)–Co–N(3)	98·5 (2)	99·1 (3)	98·9 (2)
N(2)–Co–N(4)	179·4 (2)	179·3 (3)	179·7 (2)
N(2)–Co–N(5)	90·9 (2)	90·8 (2)	90·3 (1)
N(2)–Co–C(14)	87·3 (3)	92·4 (3)	88·1 (2)
N(3)–Co–N(4)	81·6 (2)	80·6 (2)	81·1 (2)
N(3)–Co–N(5)	89·7 (2)	90·8 (2)	90·2 (1)
N(3)–Co–C(14)	89·8 (3)	92·3 (2)	92·1 (2)
N(4)–Co–N(5)	89·7 (2)	89·9 (2)	90·0 (1)
N(4)–Co–C(14)	92·1 (3)	87·0 (2)	91·6 (2)
N(5)–Co–C(14)	178·1 (2)	175·1 (2)	177·4 (2)
Co–N(1)–O(1)	121·7 (4)	124·6 (4)	123·4 (3)
Co–N(1)–C(1)	118·2 (4)	116·8 (5)	116·9 (3)
O(1)–N(1)–C(1)	120·1 (5)	118·4 (6)	119·8 (4)
Co–N(2)–O(2)	122·7 (4)	121·3 (5)	120·8 (3)
Co–N(2)–C(2)	119·0 (5)	114·9 (5)	116·4 (3)
O(2)–Co–C(2)	118·3 (5)	123·8 (6)	122·9 (4)
Co–N(3)–O(3)	123·8 (4)	122·3 (4)	123·0 (3)
Co–N(3)–C(3)	116·1 (5)	117·3 (5)	116·6 (3)
O(3)–N(3)–C(3)	120·0 (6)	120·4 (6)	120·4 (4)
Co–N(4)–O(4)	122·0 (4)	122·2 (4)	121·6 (3)
Co–N(4)–C(4)	116·9 (5)	116·1 (4)	116·9 (3)
O(4)–N(4)–C(4)	121·1 (6)	121·6 (5)	121·6 (4)
N(1)–C(1)–C(2)	112·4 (6)	112·5 (6)	112·4 (4)
N(1)–C(1)–C(5)	122·2 (6)	124·9 (7)	122·8 (4)
C(2)–C(1)–C(5)	125·4 (6)	122·6 (7)	124·8 (4)
N(2)–C(2)–C(1)	109·7 (6)	114·3 (7)	113·2 (4)
N(2)–C(2)–C(6)	122·9 (7)	122·7 (7)	121·7 (5)
C(1)–C(2)–C(6)	127·4 (7)	123·0 (7)	125·2 (4)
N(3)–C(3)–C(4)	112·4 (6)	112·9 (6)	113·1 (4)
N(3)–C(3)–C(7)	120·2 (7)	124·7 (6)	124·0 (4)
C(4)–C(3)–C(7)	127·4 (7)	122·4 (6)	122·9 (4)
N(4)–C(4)–C(3)	112·8 (6)	112·9 (5)	112·3 (4)
N(4)–C(4)–C(8)	122·9 (6)	121·4 (6)	122·2 (4)
C(3)–C(4)–C(8)	124·2 (6)	125·7 (6)	125·5 (4)
Co–N(5)–C(9)	120·2 (3)	123·3 (4)	120·6 (3)
Co–N(5)–C(13)	120·6 (3)	121·3 (4)	121·4 (3)
C(9)–N(5)–C(13)	119·2 (4)	114·5 (5)	118·0 (3)
N(5)–C(9)–C(10)	121·4 (4)	126·0 (6)	123·2 (4)
C(9)–C(10)–C(11)	116·6 (5)	119·9 (6)	118·2 (4)
C(10)–C(11)–C(17)	119·9 (5)	119·6 (5)	119·7 (4)
C(10)–C(11)–C(12)	123·3 (5)	115·2 (5)	119·3 (4)
C(17)–C(11)–C(12)	116·8 (5)	124·9 (5)	121·0 (4)
C(11)–C(17)–N(7)	175·3 (7)	178·4 (8)	177·2 (6)
C(11)–C(12)–C(13)	115·3 (5)	122·3 (5)	119·0 (4)
N(5)–C(13)–C(12)	123·6 (4)	122·0 (6)	122·4 (4)
Co–C(14)–C(15)	116·1 (5)	110·1 (4)	113·7 (4)
Co–C(14)–C(16)	114·1 (5)	121·6 (5)	117·5 (5)
C(15)–C(14)–C(16)	111·0 (6)	111·4 (6)	111·9 (6)
C(14)–C(15)–N(6)	179·2 (8)	171·4 (8)	176·6 (6)

cyanoethyl group, has very close approaches to the neighboring pyridine ligand. Such short contacts are relieved after the inversion of the configuration of the cyanoethyl group *B*. These results suggest that all the contacts around the cyanoethyl group should be taken into account in order to elucidate why only the cyanoethyl group *B* is converted into the opposite configuration.

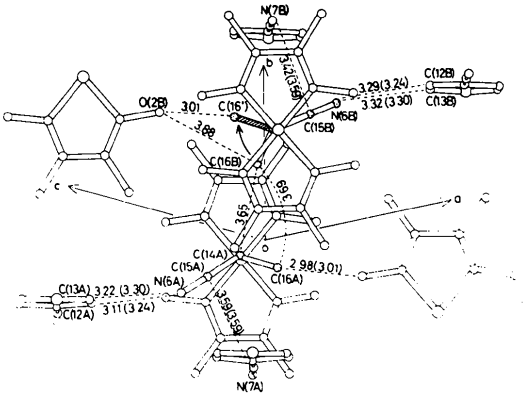

Fig. 4. Neighborhood of the two cyanoethyl groups around a pseudo inversion center viewed along the normal to the mean plane of cobaloxime *A*, and short interatomic distances (Å). At the final stage, C(16*B*) is transferred to the position C(16′).

Reaction cavity

The surroundings of the cyanoethyl group are well represented by a cavity, which is defined as a space limited by a concave surface of the spheres of the surrounding atoms, as shown schematically in Fig. 5. The radius of each sphere is taken to be 1·2 Å greater than the van der Waals radius (Bondi, 1964) of the corresponding atom. The value of 1·2 Å is the van der Waals radius of an H atom which often occupies the surface of the molecule. Thus the cavity can be a closed space. The center of any atom of the cyanoethyl group is then considered to be included in the cavity when the group makes usual van der Waals contacts with the surrounding atoms.

Fig. 6 shows stereoscopic drawings of the cavities for the two cyanoethyl groups around the pseudo inversion center at the initial stage and around the crystallographic inversion center at the final stage. The shape of the cavity at the initial stage clearly shows the

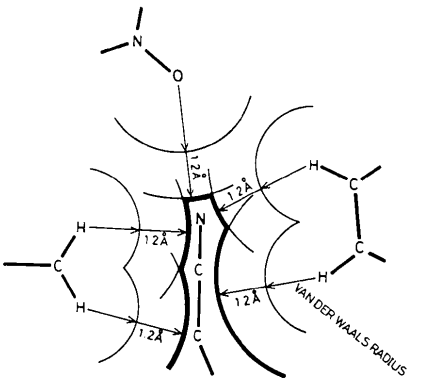

Fig. 5. The definition of the cavity for the cyanoethyl group. Each sphere is drawn at the center of each atom in the neighborhood of the cyanoethyl group with a radius 1·2 Å greater than its van der Waals one. One section is drawn in this figure.

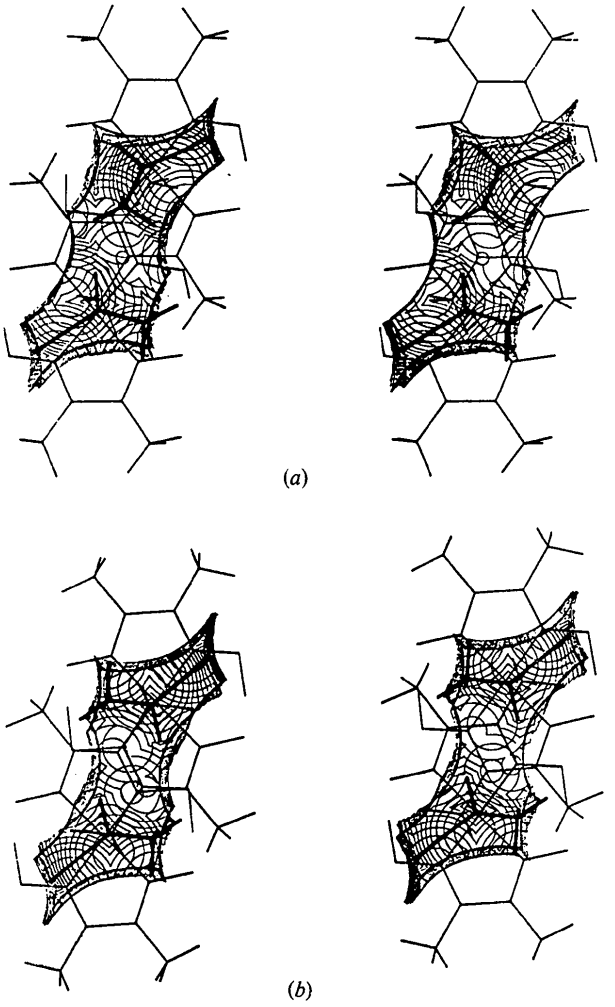

Fig. 6. (*a*) A stereoscopic drawing of the cavity for the two cyanoethyl groups *A* (lower) and *B* (upper) around a pseudo inversion center in the *R*-cn-cnpy crystal at the initial stage. The contours are drawn in sections separated by 0·10 Å. (*b*) The cavity for the two cyanoethyl groups around the inversion center at the final stage.

pseudo inversion symmetry of the packing of the surrounding atoms. When the cyanoethyl group *B* is converted to the opposite configuration at the final stage, the central part of the cavity becomes narrower. The volumes of the cavities were calculated to be 27·95 and 26·41 Å^3 at the initial and final stages, respectively, by numerical calculation. The contraction of the cavity corresponds to the decrease in volume of the unit cell.

If the cyanoethyl group *A* were converted to the opposite configuration, it would move away from the cyanoethyl group *B* in order to avoid short contacts between the methyl groups of the two cyanoethyl groups, and then the cavity would be expanded. The inversion of cyanoethyl group *A* is clearly unfavorable energetically.

For comparison, stereoscopic drawings of the cavities for the two cyanoethyl groups of the *S*-cn-py crystal at the initial and final stages are shown in Fig. 7. The two cyano groups face each other around the pseudo or crystallographic inversion center. The separation between the mean planes of the two cobaloximes is 6·34 Å and the Co···Co distance is 7·839 (1) Å at the initial stage. These distances become 6·225 (5) and 7·675 (1) Å, respectively, after the racemization. The shortening of the Co···Co distance is brought about by the approach of the cobaloxime planes for the *S*-cn-py crystal, whereas it is caused by the sliding of the cobaloxime moieties parallel to their planes for the *R*-cn-cnpy crystal.

The methyl of cyanoethyl group *B* has unusually short contacts with the pyridine ligand of the neighboring molecule in the *S*-cn-py crystal. After racemization cyanoethyl group *B* fits the cavity well. The volumes of the two cavities were calculated to be 25·58 and 26·39 Å^3 at the initial and final stages, re-

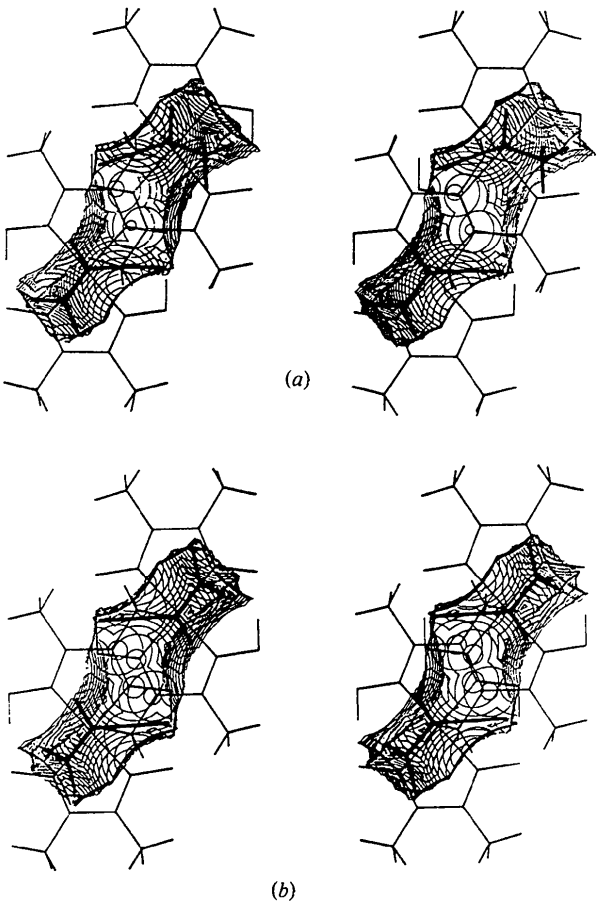

Fig. 7. (*a*) A stereoscopic drawing of the cavity for the two cyanoethyl groups *A* (lower) and *B* (upper) around a pseudo inversion center in the *S*-cn-py crystal at the initial stage. The contours are drawn in sections separated by 0·10 Å. (*b*) The cavity for the two cyanoethyl groups around the inversion center at the final stage.

spectively. Since the volume of the unit cell also decreases in the course of racemization, closer packing must occur elsewhere than around the cyanoethyl groups for the *S*-cn-py crystal. If cyanoethyl group *A* were converted to the opposite configuration, the cavity would be expanded to a large extent to avoid the short contacts between the methyl and cyano groups. It is noteworthy that the cavity at the final stage has nearly the same volume as the corresponding one of the *R*-cn-cnpy crystal.

Relationship between the reaction rate and the cavity

Although inspection of the cavity for the two cyanoethyl groups around the pseudo inversion center is useful for elucidating why only cyanoethyl group *B* is converted to the opposite configuration, it is advantageous to compare the cavity for one cyanoethyl group with that of the other. Fig. 8 shows the cavities for cyanoethyl groups *A* and *B* of the present crystal, projected along two axes. The shapes of the cavities clearly indicate that the inversion of cyanoethyl group *B* easily takes place. The final cavities are also shown in Fig. 9, in which the projections along the long axis of cobaloxime are omitted since they are nearly the same as the initial ones.

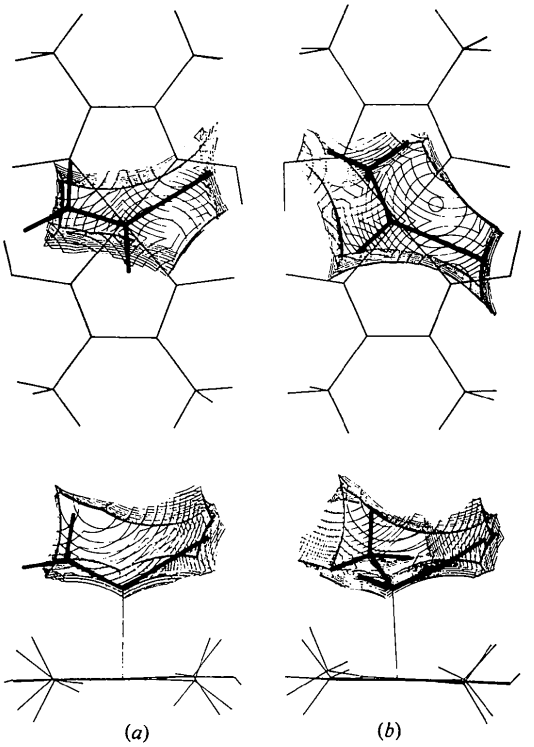

(*a*) (*b*)

Fig. 8. (*a*) Two projections of the cavity for cyanoethyl group *A* viewed along the normal to the cobaloxime plane and along the long axis of the cobaloxime. The contours are drawn in sections separated by 0·10 Å. (*b*) The cavity for cyanoethyl group *B*.

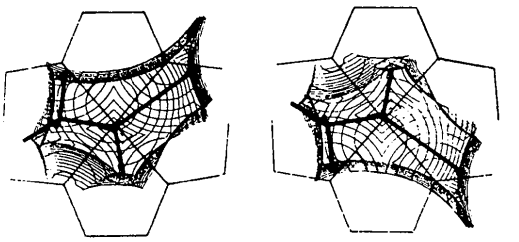

(*a*) (*b*)

Fig. 9. The cavities for the cyanoethyl group at the final stage, viewed along the normal to the cobaloxime plane. (*a*) and (*b*) correspond to *A* and *B*, respectively, in Fig. 8, and are mirror images of each other. The contours are drawn in sections separated by 0·10 Å.

Table 5. *Volumes of the cavities* (Å^3) *for the initial A and B and the final A′ cyanoethyl groups, and rate constants* [k(s^{-1})] *in crystals of R-cn-cnpy and S-cn-py*

	R-cn-cnpy	*S*-cn-py
A	7·97	8·89
B	10·37	11·34
A′	10·52	10·52
(*A* + *B*)*	27·95	25·58
(2*A′*)†	26·41	26·39
k	1·65 × 10^{-6}	2·83 × 10^{-6}

* The cavity for the two cyanoethyl groups *A* and *B* around a pseudo inversion center at the initial stage.

† The cavity for the two cyanoethyl groups *A′* around an inversion center at the final stage.

The volumes of the cavities are given in Table 5, in which the values for the *S*-cn-py crystal are also shown. Cyanoethyl group *B*, the reactive group, has a greater volume than cyanoethyl group *A* in each crystal. Table 5 also lists the reaction rates of the two crystals. The larger the volume of the cavity for the reactive group, the greater the reaction rate is.

For the *R*-cn-*S*-mba crystal, every cyanoethyl group is converted to the disordered racemate by X-ray exposure at 293 K. The racemization, however, was no longer detectable below 173 K. The volumes of the cavities at 293 and 173 K were calculated to be 14·53 and 12·95 Å^3, respectively. Recently, another type of order-to-order racemization has been found in a crystal of [(*R*)-1-cyanoethyl](4-methylpyridine)cobaloxime (Uchida, Ohashi, Sasada & Ohgo, 1982). The cavity for the reactive group also has a greater volume than that for the non-reactive group.

In summary, it is clear that the reactivity or reaction rate has a positive correlation with the volume of the cavity for the cyanoethyl group. However, the fact that the volume of the cavity for the non-reactive cyanoethyl group in *R*-cn-*S*-mba at 173 K is larger than that for the reactive *B* group in the present crystal suggests that the threshold value for the racemization may be different for the different mechanisms.

This work was supported by a Grant-in-Aid for Scientific Research from the Ministry of Education, Science and Culture, Japan.

References

BONDI, A. (1964). *J. Phys. Chem.* **68**, 441–451.

International Tables for X-ray Crystallography (1974). Vol. IV, pp. 71–151. Birmingham: Kynoch Press.

KURIHARA, T., OHASHI, Y. & SASADA, Y. (1982). *Acta Cryst.* B**38**, 2484–2486.

MAIN, P., HULL, S. E., LESSINGER, L., GERMAIN, G., DECLERCQ, J. P. & WOOLFSON, M. M. (1978). *MULTAN* 78. *A System of Computer Programs for the Automatic Solution of Crystal Structures from X-ray Diffraction Data.* Univs. of York, England, and Louvain, Belgium.

OHASHI, Y. (1975). Unpublished. Original *HBLS* program by T. ASHIDA.

OHASHI, Y., KURIHARA, T., SASADA, Y. & OHGO, Y. (1981). *Acta Cryst.* A**37**, C-88.

OHASHI, Y. & SASADA, Y. (1977). *Nature (London)*, **267**, 142–144.

OHASHI, Y., SASADA, Y. & OHGO, Y. (1978*a*). *Chem. Lett.* pp. 457–460.

OHASHI, Y., SASADA, Y. & OHGO, Y. (1978*b*). *Chem. Lett.* pp. 743–746.

OHASHI, Y., YANAGI, K., KURIHARA, T., SASADA, Y. & OHGO, Y. (1981). *J. Am. Chem. Soc.* **103**, 5805–5812.

OHASHI, Y., YANAGI, K., KURIHARA, T., SASADA, Y. & OHGO, Y. (1982). *J. Am. Chem. Soc.* **104**, 6353–6359.

SHELDRICK, G. M. (1976). *SHELX* 76. Program for crystal structure determination. Univ. of Cambridge, England.

UCHIDA, A., OHASHI, Y., SASADA, Y. & OHGO, Y. (1982). In preparation.

Acta Cryst. (1983). B**39**, 61–75

Experimental *versus* Theoretical Charge Densities: a Hydrogen-Bonded Derivative of Bicyclobutane at 85 K

BY M. EISENSTEIN AND F. L. HIRSHFELD

Department of Structural Chemistry, Weizmann Institute of Science, Rehovot, Israel

(*Received* 10 *September* 1981; *accepted* 5 *May* 1982)

Abstract

The charge deformation density in 1,3-diethylbicyclobutane-*exo*,*exo*-2,4-dicarboxylic acid has been mapped by least-squares refinement against low-temperature X-ray data extending to $2 \sin \theta/\lambda = 2{\cdot}73$ Å^{-1}. Results agree semi-quantitatively with *ab initio* calculations on bicyclobutane, ethane, and formic acid cyclic dimer. Experimental and theoretical deformation densities show similar bond bending in the bicyclobutane nucleus, similar net charges and moments of corresponding atomic fragments, and a similar charge distribution in the hydrogen-bonded carboxylic acid. Wide variability in C—C bond lengths and dihedral angle in several substituted bicyclobutanes implies great flexibility for this strained system. [Crystal data at 85 K: $C_{10}H_{14}O_4$, $P2_1/c$, $a = 7{\cdot}627\ (2)$, $b = 9{\cdot}306\ (2)$, $c = 16{\cdot}928\ (6)$ Å, $\beta = 121{\cdot}53\ (3)°$; $R = 0{\cdot}0917$, $R_w = 0{\cdot}0650$ for 9103 reflections.]

Experimental charge density studies by means of accurate X-ray diffraction measurements have been found capable, in favorable circumstances, of yielding detailed deformation density maps of at least semi-quantitative significance. One way of testing the reliability of such maps is by comparison with charge densities derived from *ab initio* calculations. Such a comparison provided strong support for the experimental static deformation density of diformohydrazide (Eisenstein, 1979) derived from the low-temperature X-ray data of Hope & Ottersen (1978). Further comparisons of the same sort are needed to establish the conditions leading, on the one hand, to reliable experimental charge densities and, on the other, to accurate theoretical maps. The present study applies such a test to the experimental deformation density of 1,3-diethylbicyclobutane-*exo*,*exo*-2,4-dicarboxylic acid (DBDA). It thus combines an investigation of the charge distribution in a particular strained molecule of great chemical interest with a contribution to the methodology of experimental and theoretical charge density studies.

The DBDA molecule comprises a bicyclobutane nucleus substituted at all four C atoms. The bridge atoms carry ethyl substituents while the other two ring atoms have carboxylic acid substituents in the *exo* positions. These carboxyl groups form cyclic hydrogen-bonded links with neighboring molecules related by a crystallographic glide plane. The several portions of the molecule may be compared with the three model compounds bicyclobutane, ethane, and formic acid

0567-7408/83/010061-15$01.50